KU LEUVEN

FACULTY OF ENGINEERING TECHNOLOGY

DE NAYER (SINT-KATELIJNE-WAVER) CAMPUS

Vision-based automatic tool-wear inspection system

Lars DE PAUW

Promotor: Prof. dr. ir. T. Goedemé

Co-promotors: Dr. ing. D. Hulens
Dr. ir. T. Jacobs

Master Thesis submitted to obtain the degree of
Master of Science in Engineering Technology:
Electronica-ICT major in ICT

Academic Year 2020 - 2021

Contents

List of Figures

List of Tables

List of symbols

Maak een lijst van de gebruikte symbolen. Geef het symbool, naam en eenheid. Gebruik steeds SI-eenheden en gebruik de symbolen en namen zoals deze voorkomen in de hedendaagse literatuur en normen. De symbolen worden alfabetisch gerangschikt in opeenvolgende lijsten: kleine letters, hoofdletters, Griekse kleine letters, Griekse hoofdletters. Onderstaande tabel geeft het format dat kan ingevuld en uitgebreid worden. Wanneer het symbool een eerste maal in de tekst of in een formule wordt gebruikt, moet het symbool verklaard worden. Verwijder deze tekst wanneer je je thesis maakt.

b	Breedte	$[mm]$
A	Oppervlakte van de dwarsdoorsnede	$[mm^2]$
c	Lichtsnelheid	$[m/s]$

List of Acronyms

WC Wolfram Carbide

Convolutional Neural Network (CNN)

Transfer learning TL

Stochastic gradient descend SGD

Weights and biases wandb

Graphics Processing Unit GPU

Chapter 1

Introduction

The steel industry is a big industry in the world and provides 2.5 million jobs across Europe according to the European commission. Due to high labor costs in western Europe and more specific in Belgium labour costs are about 40% above the average of labour costs in Europe. For this reason production and manufacturing costs should lower to be able to compete with other companies around the world.

For this thesis we focus on metal carving which is done by spinning a spindle over the metal work piece that carves away material. This spindle holds inserts as seen in Figure 1.1 where a top and side view of the insert are provided. A full assemble of the tool and the insert can be found in Figure 1.2. The inserts are kept in place with a screw for easy removal and replacement and are made of different compositions of Wolfram carbide. After creation they get a coating on the outer layer to provide extra strength and more capabilities to cut different materials.

(a) Top view

(b) Side view

Figure 1.1: Images of the examined carbide tool inserts. The red square marks the area of interest for the wear prediction.

The cutting part on the corner of the insert - as marked on Figures 1.1a and 1.1b with a red square - will wear when the work piece is carved and will result in a bad finish on the actual product which can be referred to as surface roughness. To prevent the formation of surface roughness the tool inserts must be replaced before they are worn to much. For this replacement there are two policies

Figure 1.2: Milling tool with one insert in place.

used in the industry today:

1. Check the inserts when a work piece is finished.
2. Replacing all inserts on set time intervals (e.g. every 30 minutes).

Although option number one will optimize the lifespan of the inserts, it is very time consuming and labor intensive. Option number two is less labor intensive and thus less time consuming but will produce a lot of waste in those inserts. Having safety levels there will be a lot of inserts thrown away even when they are still usable.

What does a worn insert look like? This is shown in Figure 1.3 which is a close up from the area marked with a red square from Figure 1.1b. Figure 1.3 gives examples of a barely used insert and one of an insert which is unusable due to the high wear.

The goal for this master thesis is to create a direct measurement method to quantize the tool wear on these inserts. From this goal the research questions can be extracted: ”How can tool wear on carbide inserts be quantized by using a direct method?”. ”How can a vision set up be implemented in a production line?” ”What should the vision set up look like?” ”What computer vision algorithms perform best for this task?” For this report however only the beginnings are given where a highly adjustable setup is created as well as some datasets and an algorithm to measure the performance of a specific setup.

The problem will be split up into two main parts:

- Creating a camera setup to capture images of the inserts.
- Create a vision algorithm to process the images and output the tool wear.

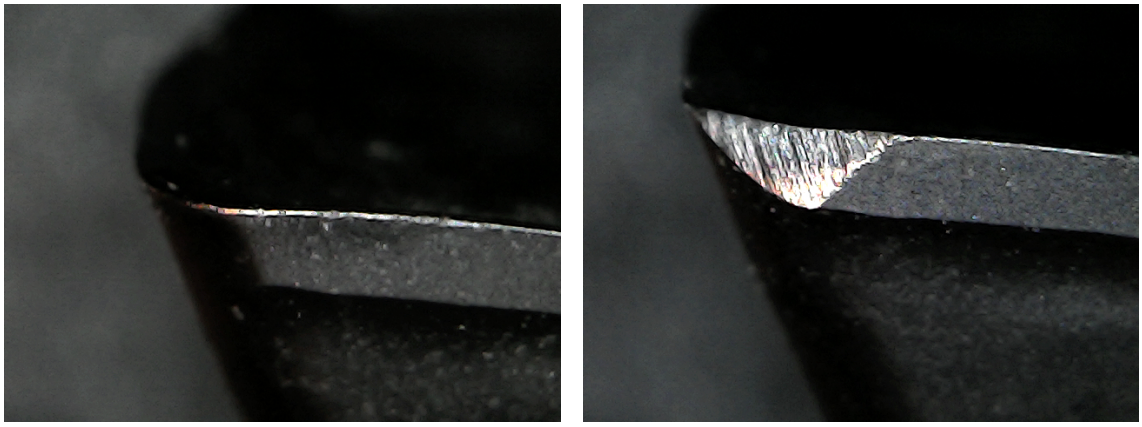

(a) Barely used carbide insert. **(b)** Worn carbide insert.

Figure 1.3: Illustration of a good and a worn insert.

First the state of the art for this problem will be discussed along with some extra literature information on the whole of this problem in chapter 2. The implementation will be handled next in chapter 3 where the process of building a solution is bespoken. The results on the setup, and the generated datasets will be discussed in chapter **??**. After this a conclusion is written in chapter 5 and the research questions are revisited.

Chapter 2

Literature review

2.1 State of the art

In this research area there are a lot of enhancements taking place. The industry 4.0 makes it easier to collect data and process this into usable numbers. With this indirect measured sensor data a lot of research is done on the prediction of tool wear. For example Ma et al. (2020) uses cutting force as input for a Convolutional Neural Network (CNN) which predicts the tool wear. Li et al. (2013) proposes a setup which will detect the tool wear in-line and creates an overview of the tool life with three different tool wearing categories namely nose wear, flank wear and crater wear. The wear is displayed for different machining times. Li et al. (2013) also creates an overview of tests on different materials and different coatings, this gives the reason why it is important to detect tool wear in an early stage to produce as many good products as possible

Cerce et al. (2015) provides a way to measure tool-wear with a 3D laser profile sensor. This would be more accurate since more data is available to the algorithms. Here tool-wear is divided in two categories: premature tool failure and progressive tool-wear. The premature tool failure ”mostly occurs as sudden and unpredictable breakage of the cutting edge” these types of error’s wont be detected. The progressive tool-wear on the other hand is easier to predict and measure. Here the inability of measuring wear profiles in depth is the main disadvantage of direct measuring methods. The results of this paper are really good, they detect the numbers on the crater wear and nose wear of the tool. This with an accuracy of 1 micrometer.

A remarkable study is made by Pagani et al. (2020) who uses the chips cutoff by the tool to predict the tool wear.

Although many researchers choose for indirect measurement methods there are some that use direct methods like Ambadekar and Choudhari (2020). They use a microscope to perform off-line tool wear classification in three categories. What they provide is a very similar research as the one done for the setup verification model. We will go even further than classification by also predicting the exact flank wear in micrometer. The architecture used by Ambadekar and Choudhari is Resnet 50 which will also be tested to compare with this study findings. The accuracy achieved is 87% for the three classes.

Schmitt et al. (2012) discribes a way of using machine vision to inspect flank wear on cutting tools. The process they use is very labor intensive and should be redone when inspecting a new tool. Their steps are ”image acquisition, tool edge detection, highlighting wear region, feature extraction, wear type classification and finally wear measurement.” In our paper we will try to make this process a lot simpler by using deep neural networks which will be trained on different tool types. But we will need more labeled data to be able to perform such a task which may be expensive to create. An accuracy of 7.5 micrometer is achieved.

2.2 Light reflections on the tools

To get a better understanding of the reflections of the tool inserts we take a look at how the inserts wear over time and what characteristics they have.

2.2.1 How does the tool wear?

This base material will mostly be Wolfram carbide (WC) due to its strength and heat resistance. The same material can also be referred to as tungsten carbide. This base material is covered in a coating to provide extra strength and durability. Gu et al. (1999) Creates an overview of the different wear types with or without coating and the durability under different testing conditions. Figure 2.1 shows how the material is coated and not yet used. The wear of the tool begins with wear on the coating and goes right through the the coating in the base material of the tool. Figure 2.2 Shows the two types of wear seen on the surface of the inserts. Figure 2.2a shows the result of a slow spinning mill where the tool chips off. Figure 2.2b shows the wear on an insert which was used under high speeds and where the worn area is flat but not perpendicular to the rake face. This will have to be considered for the light set-up to be able to handle both wear types.

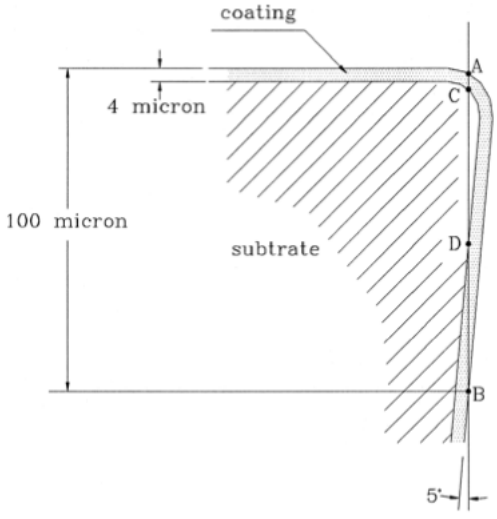

Figure 2.1: Construction of the Tool insert with coating. Figure from (Gu et al., 1999)

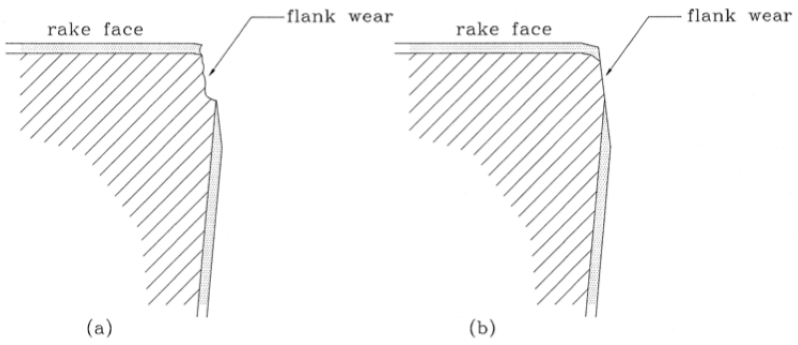

Figure 2.2: Two wear types: (a) Step between substrate and coating. (b) flat wear not perpendicular to the rake face Figure from (Gu et al., 1999)

2.2.2 Surface of the insert

WC typically has a grain size of 0.5 μm to 2 μm which is bonded with cobalt that acts as cement between the WC grains. This declares the name of cemented carbides.

The next paper is good to get an overview of the light reflection seen in different types of materials and even multi layered tools where Caicedo (2019) researched the reflectance of coating layers on tool inserts. Here is described that the best reflection occurs at the highest wavelength. This translates to the visible color red and means that the reflection should be the optimal when the lighting is on the top of the spectrum of the camera.

2.3 Vision algorithms

In this section a brief background will be given for the used software and computer vision algorithms. Starting with a listing of different frameworks and after that some Neural network architectures will be explained.

2.3.1 Frameworks

There are many frameworks to perform computer vision tasks and make it as easy for the user to get a lot done in a short amount of time. In what follows the different frameworks used in this thesis are listed and shortly documented.

- Fast.ai (J, 2020)
- Keras (I, 2020)
- PyTorch (Adam et al., 2020)

Basnet et al. (2019) provides an overview of different deep learning frameworks, a short summary is given below. Fast.ai provides a very high level programming experience designed to make deep

learning very easy. We found this to be too high level which would affect the customizability of the algorithms. Keras is also a high level framework which works with very little programming which is designed for experimenting. PyTorch leaves a little more room for customization. This is the reason PyTorch was used for the most of this thesis.

2.3.2 Architectures for set-up verification

Starting from a very small amount of test material (inserts) for the creation of a vision set-up, it is nessecary to choose some relevant deep learning network architectures that perform well with small datasets. The results of the image procession will be used to compare different vision setups. The dataset consists of a little less than 300 images. This constraints the choice of architectures to the ones with very little training parameters since there are not much input images to which the parameters can be trained. In the next sections are some well-known architectures that are used for this determination.

First an algorithm must be found that can quickly confirm whether a setup is good or not. This will be done by taking pictures from different camera positions with the same lighting. After this the images go trough a simple model and the output is verified with a test set.

The first algorithm will be Resnet 18 since this is known to to perform well with less parameters and deeper architecture. Khan et al. (2020) extensively describes most available CNN architectures a few of them are used and repeated underneath for a better understanding of the architectures.

2.3.2.1 Resnet18

First define what Resnet (He et al., 2016) means than dig deeper into the Resnet18 architecture.

Resnet is a deep residual neural network that can reach deeper networks without affecting the complexity of the network. What means the amount of parameters or the complexity of the training will not increase much when extra layers are added to the model. The depth of the network plays an important role in the performance.

Figure 2.3 gives an overview of the important building block which lead to the success of Resnet. Rather than just stacking layers on top of each other, they provide shortcut connections that skip one or more layers. These shortcut connections perform identity mapping where the output of the previous blocks are added to the output of the stacked layers. This doesn't add extra complexity to the model but allows for more layers to be stacked on top of each other.

Figure 2.4 displays a summary of all blocks in the network architecture of Resnet 18. The arrows represent shortcut connections over a few layers. The blocks represent a 3x3 convolution layer where a 3 by 3 grid goes over the previous output and calculates the product with a weight matrix which is updated during training. These calculations provide a new input for the next layer. The total parameter count for this architecture is 11 million. This seems quite a lot but is actually not much. This will later be compared with other network architectures in section 2.3.3.

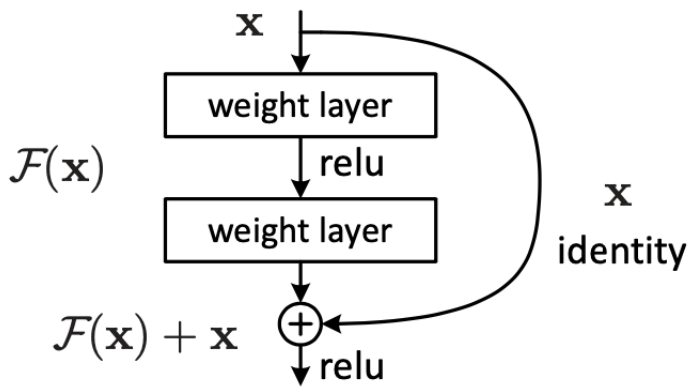

Figure 2.3: a building block for Resnet architecture

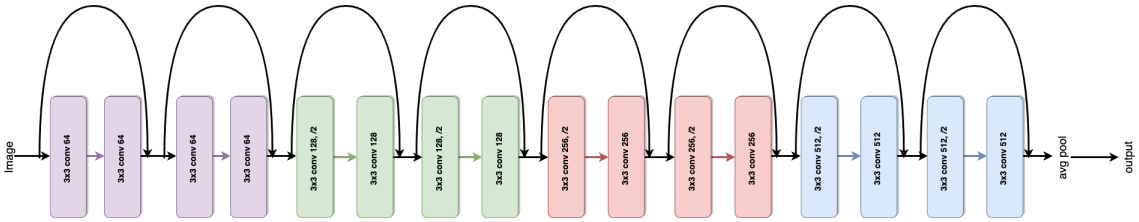

Figure 2.4: Summary of Resnet 18 architecture

2.3.2.2 VGG11_bn

VGG is a network architecture found by Simonyan and Zisserman (2015) it was designed to get better results at the famous imagenet classification task and does this by using a deeper structure with smaller convolution filters. The original architecture was designed for large scale image classification tasks but will be used for a small dataset in this thesis where VGG is used with 11 layers instead of the original 19 layered architecture.

The bn stands for batch normalisation which will normalize the output of previous activation layers before passing it on to the next layers. The normalisation will be calculated on every batch instead of the whole dataset.

2.3.2.3 Alexnet

Alexnet by Krizhevsky et al. (2017) was one of the first to implement deeper structures in the before known CNN architectures. The implementation of deeper network led to over fitting which was countered with including dropout in the fully connected layers. This makes the model more stable even with more layers. In the time Graphics processing units (GPU's) where not as developed as today so the initial architecture consisted of two parallel paths which could run on two separate GPU's.

2.3.2.4 Densenet 121

ToDo

2.3.2.5 Squeezenet

ToDo

2.3.3 Overview of important numbers

Parameters and depth for all architectures are given in table 2.1. The amount of parameters and the depth define the complexity of the architecture. Where more layers and more parameters increase the complexity.

Table 2.1 Parameters and depth in layers for every model accuracy

Model name	parameters (million)	depth (layers)
Resnet 18	11.7	18
VGG11_bn	123.6	11
Alexnet	61.1	8
Densenet 121	7.9	121
Squeezenet	1.2	10

2.3.4 Other architectures for small datasets

Very little datasets are available for this problem so all data used in this thesis will be self created. For this reason there are very few images to train and test algorithms on. In what follows are some interesting network architectures given for small dataset image classification. These can later be adjusted to perform image regression tasks.

A first architecture is proposed by Chandrarathne et al. (2019). They compare training a five layered neural network from scratch with using transfer learning on the imagenet dataset. The findings where that transfer learning could increase the testing accuracy by 10% on small datasets.

Xu et al. (2019) proposes a so called SDD-CNN what stands for small data driven convolution neural network. This was used for the inspection of roller bearings. A preprocessing method called label dilation is used for dataset imbalance because there is a big imbalance in amount of positive and negative examples. This label dilation method generates random classes where the amount of items per class after dilation equals the amount of items in the biggest class before dilation. For the roller bearings there are 300 samples per class. After preprocessing the images are augmented to extend the dataset in a controlled way using semi-supervised data augmentation. This process is done by cropping the worn area of the bearing rather than center cropping. Then four networks are trained with the received data. These networks are:

1. Squeezener v1.1
2. Inception v3
3. VGG-16
4. ResNet-18

The findings of the research are that inception v3 performed best for this small dataset when used with transfer learning.

Chapter 3

Implementation

3.1 Camera setup

Carbide tool inserts are not yet items that are much researched so there are no big datasets that can be used to train and test algorithms on. Therefore a new dataset must be created with worn tool inserts. For the creation of the dataset a setup is created. This setup consists of three different parts:

1. A tool holder which will provide the same position for the tool for every picture
2. A mount for the microscopic camera which is easy to finetune
3. Some lighting solution that provides the right angle of light to the tool insert.

3.1.1 Design of a tool holder

The tool holder will be the most important part of the setup since this part will be holding the tool insert where every imperfection will be seen on the output images. The requirements for this holder are that the inserts should be easy to remove and to replace. It should be almost not visible to the camera.

3.1.1.1 First tool holder

All tool holder prototypes where 3D printed. A first holder was made to check how the lighting would be transferred to the camera. This was put in a simple setup with a desk lamp and a socket which kept the insert at an angle of 40°. The socket can be found on Figure 3.1. This showed potential in the current setup as seen in Figure **??**. The tool wear is nicely indicated with the reflections of the light.

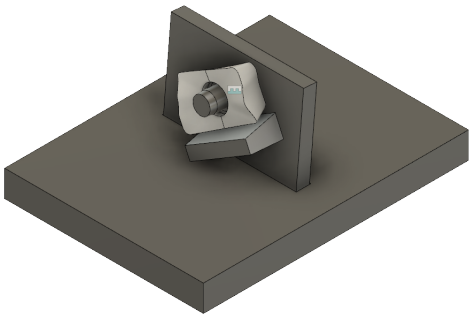

Figure 3.1: First design of a tool holder oriented at an angle of 40 °to the camera.

3.1.1.2 Wheel holder

The previous first tool holder was good for taking a sample picture of an insert but isn't scalable to take pictures of a few hundreds of inserts. To be able to quickly create a lot of photos in a consistant manner, a wheel is designed to mount 20 inserts at once. With the use of a stepper motor and a fixed camera and lighting setup, the process of taking images is automated for every 20 tools. The holder is 3D printed so a few wheels can be made to be able to swap the wheels with new inserts for an efficient dataset creation.

The first design of this wheel holder can be seen in Figure 3.2. Here everything is printed in one piece. The inserts are kept in place with brackets that go over the cutting edge of the insert. This wasn't ideal since the sharp edges of the insert would clamp in the bracket what made it very hard to remove the tools and didn't comply with the easy removal constraint.

For this reason a second wheel was designed which was a little more flexible and made the process of inserting and replacing tools a lot easier by providing a clip which was printed and added to the wheel separately. Figure 3.3 shows the full assembly of this second wheel holder.

In the wheel there are holes in which the clips fit. The center hole is as big as the hole in the inserts. This keeps the insert from moving when the clip is on. The slads between the holes are made to fit the insert perfectly so this doesn't rotate around the axis of the clip. On the clip there is an extra long middle tube that makes it easier to push the clip with the insert out of the wheel.

The printing of these wheels was very difficult since it was with another material as we were used to and the print wouldn't stick to the print bed. This made a few bad runs and hours of wasted printing time. At the end 8 wheels of this are printed correctly and were used to create the datasets which will be covered in section 3.2.

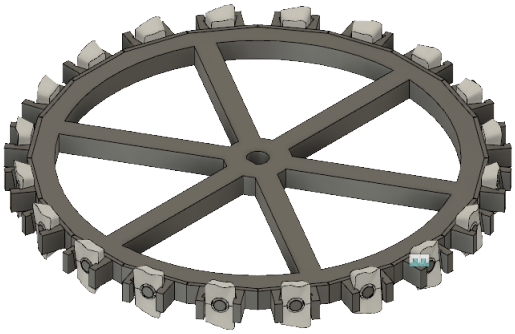

Figure 3.2: First design of wheel holder with inserts mounted in place.

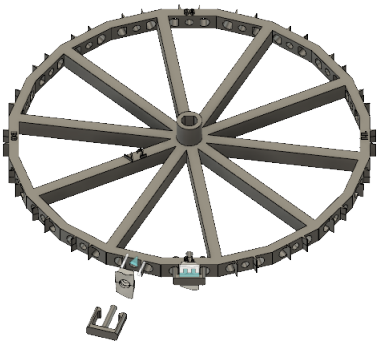

Figure 3.3: Second wheel holder with clip and insert.

3.1.2 Design of a camera mount

In this page the camera mount will be discussed along the design process of the setup Since the camera mount provided by the factory was not up to the task of taking consistent pictures and controlling the camera position precisely, a new camera mount was designed. For this task some 20mm by 20mm aluminium profiles where used as a base for the stand. On that stand an assembly of 3D printed parts where mounted to be able to rotate the camera around two different axis.

A render of the full assembly of this new camera mount can be found in Figure 3.4.

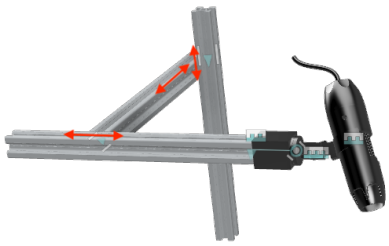

Figure 3.4: A render of the camera mount with the given movement options.

3.1.3 Light configuration

In order to test different lighting options there must be a simple to configure lighting solution. Which is configurable in both color and light direction to create a maximum reflection of the wear area into the camera lens. This is achieved with single led adressable light.

Multiple different light sources where tested as listed underneath. Some worth noticing are declared after.

1. Warm white led desk Lamp
2. Long hard white led strips
3. single led adressable RGB led strip
4. Multiple single led adressable RGB strips
5. USB microscope camera light

3.1.3.1 Desk Lamp Test

As an initial setup to test the camera and be able to see the effects of lighting on the image this setup was created and a desk lamp was used for the lighting as seen in Figure 3.5.

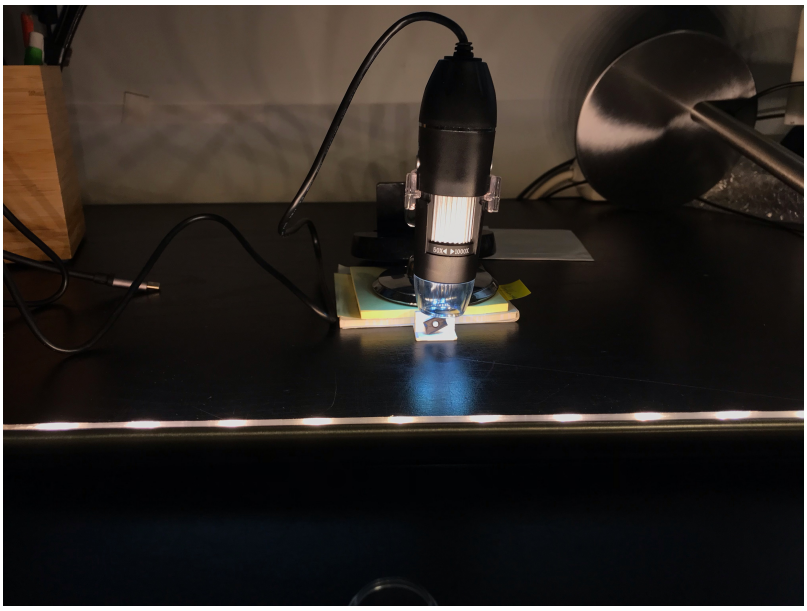

Figure 3.5: Desk lamp setup for initial testing.

This setup was using the top light of the camera. This light was good to be able to adjust the camera. Without the light, the errornous places where more visible. But the desk lamp had to much brightness and didn't leave enough room for adjusting different settings. For this reason other lighting options where explored.

From this setup it can also be seen that the lighting on the background is important. Figure 3.6 shows a picture of the tool with desk lamp lighting without blocking the light from the background. Here we can see that there is a bright white background behind the tool.

The result of this is shown in Figure 3.7 where the light is blocked off of the rest of the tool and only the errornous part is lightened. This would be a good start for creating a dataset.

The color of the desk light set a good gradient of bad vs good sets. White areas are worn very hard while orange is not worn that hard.By tilting the lamp up and down in a horizontal way, all the areas where ligthtend.

3.1.3.2 White Led Strips

A second lighting contition created is the lighting with 3 the same led strips controllable with a raspberry pi. For the purpose of this test a small electric circuit is created to control these strips since they use more power than the raspberry pi can deliver (rpi, 2020). An overview of the test circuit can be found in Figure 3.8. A potentiometer was used to control the voltage over the led strip in order to control the brightness.

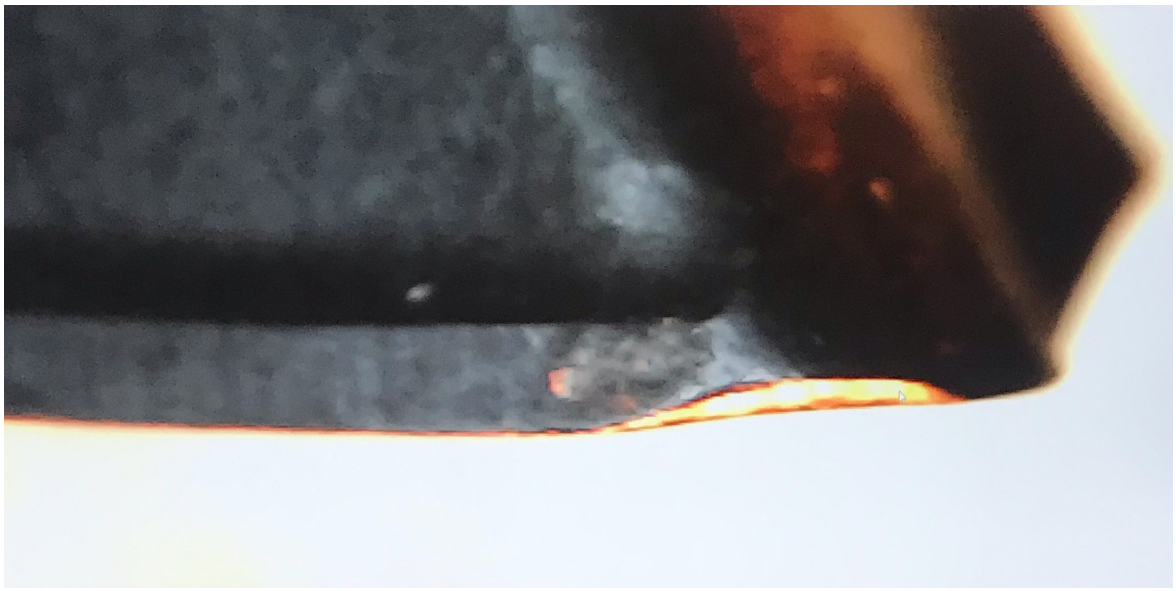

Figure 3.6: Desk lamp setup without shadowing the background.

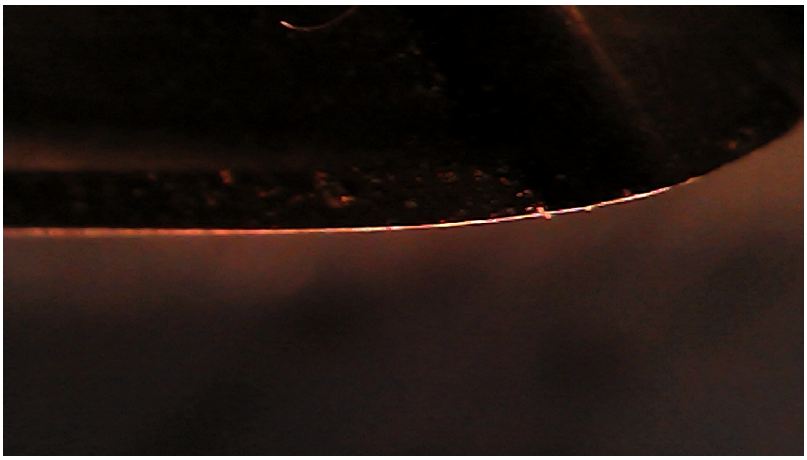

Figure 3.7: Desk lamp setup with shadowing the background.

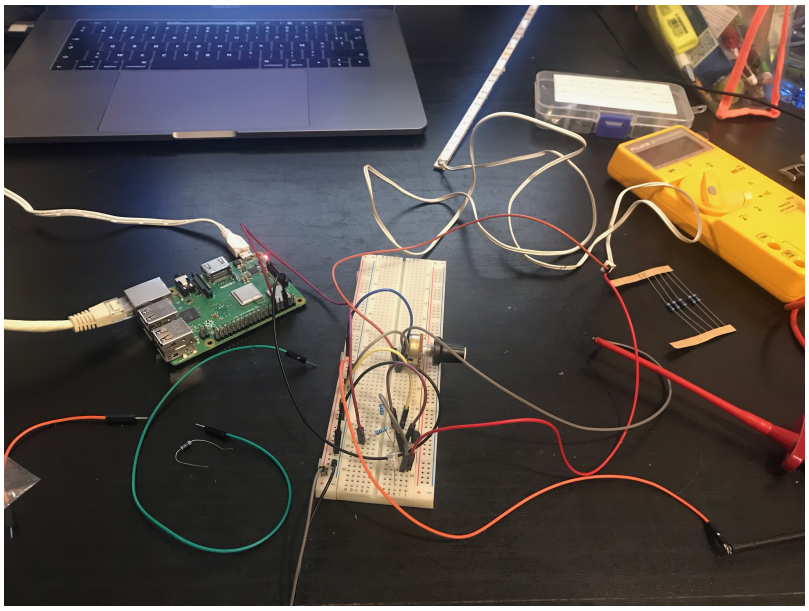

Figure 3.8: White led strips test circuit.

3.1.3.3 Adressable Color Changeable Led Strip

A third option of lighting is playing with the colors of the light. to archieve this a setup will be created with a single adressable light strip where the color and led can be freely chosen. To assign a color which works best; a study is made to find the wavelengths where the light reflects most on the used materials of the tool. This can be found in section 2.2

From all these settings the single adressable led strip was chosen due to the amount of options this creates. This choice is documented in future tests which will be discussed in section ..... . The led strip were mounted on metal strips which provided high adjustability. This made it possible to get lighting on different parts of the tool insert what makes later research easier. In Figure ..... the light configuration is displayed for a partly worn tool.

insert tool with reflection

As seen on this render there are a lot of options with this setup. Each led strip can rotate and fifteen leds can be individually set to a color. The arc keeps a consistent distance between the led and the insert.

3.2 Datasets

A separation is made between hand made datasets and automated datasets because they take a very different approach and produce very differing results.

3.2.1 Handmade datasets

The following datasets where produced using a microscopic camera to take pictures of single inserts all placed under the camera by hand. The initial dataset is produced by Sirris.

3.2.1.1 initial dataset

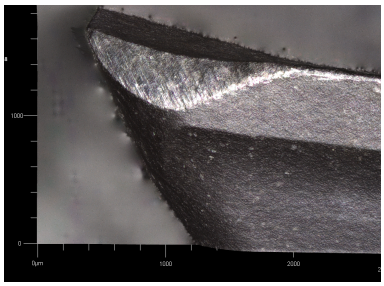

Figure 3.9: Example of initial dataset

The dataset given where taken with a microscopic camera at Sirris. These images were in good lighting conditions for the measurement, but had a lot of extra ”unwanted” features on it. The background was very like the wear and the rest of the tool insert.

Every insert that was measured had a little mark on one side to mark the a and b side of the insert. An example of this mark is given in Figure 3.10. Sadly the information about what the marker meant is lost. To find the corresponding values, the inserts where once again put through a microscopic camera and the new pictures where compared against the old ones.

Figure 3.10: Marked side of an insert.

3.2.1.2 Second handmade dataset

A second dataset was made to compare the pictures with the previous dataset. This is done to verify the images and the results and to determine what the markings on the inserts mean. This dataset handles the first 5 batches labeled with 00x. For this dataset a setup was made where the insert is placed on its side on a black background with the microscope camera vertical above the insert. Only the light from the camera was used.

Figure 3.11: Bulled mark marked on the top view of an insert.

During the creation of this dataset the inserts where labeled with bullet or no bullet. What we mean by bullet is marked on Figure 3.11. Now all labels have a value, whether the side of the insert is marked and it is noted if the side had a bullet mark. Later on this bullet can be used as an universal identifier of the correct sides.

symbol	explanation
s	side with marker line
n	side without marker line
batch number	number specified on the box in which the inserts are kept
insert number	number specified inside the box; this goes from 1 to 10 per batch

The naming of the dataset is as follows:

b_<batch number>_p_<plate number>_<identifier of side>

After looking at the pictures in Figure 3.12 it can be confirmed that the two images correspond and that the 'b' side of the inserts is the side with the mark on.

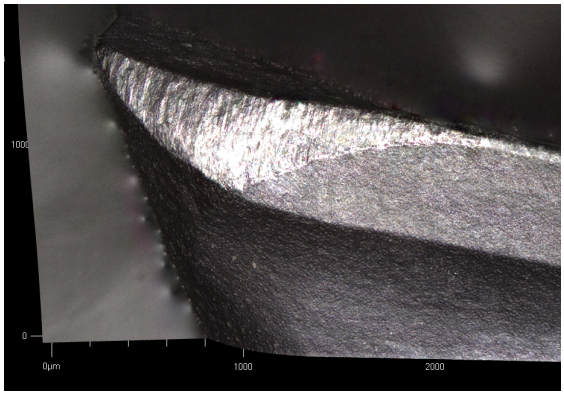

(a) Image from the first initial dataset.

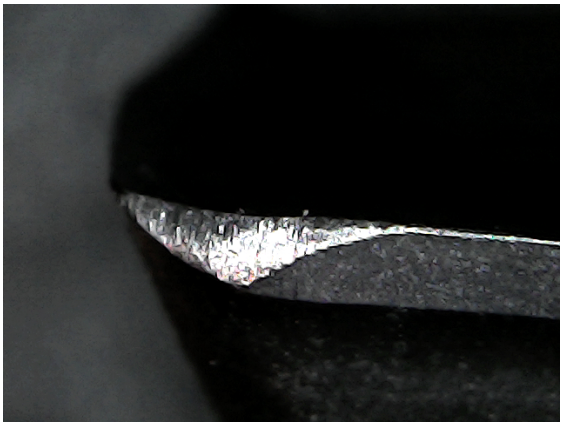

(b) Image from the second handmade dataset.

Figure 3.12: Comparison of the same insert 19 from batch 5 the side with marking.

3.2.1.3 second initial dataset

The second initial dataset was made with the inserts from batches 11 to 19 labelled with 01x. Here the images where taken with the same microscope as the first initial dataset but instead of photographing only the one insert at a time, two inserts are photographed per shot. Since the photo's where labelled with two inserts at a time, the images taken where not relevant for the data processing and were not saved.

3.2.2 Automated datasets

The hand made datasets are not scalable for a hundred or even a thousand inserts so a way of automatically creating datasets was researched in 3.1. With those things figured out a program was written to control the setup and save the taken images in a logical order. This process took a lot of test tries to find out a good camera position which will be handled first. After that the two created datasets will be discussed.

3.2.2.1 Camera position

In this section the best camera position will be defined for the creation of the dataset. Top view as well as side view will be tested.

Side camera position For these tests the first four plates of batch 004 are used. The lighting is red light coming from the addressable led strips that shine from different directions. This setup can be seen on Figure 3.13.

Figure 3.13: Camera setup for testing the camera angle.

Due to the problems with the arduino communications described here the first dataset wasn't suc-

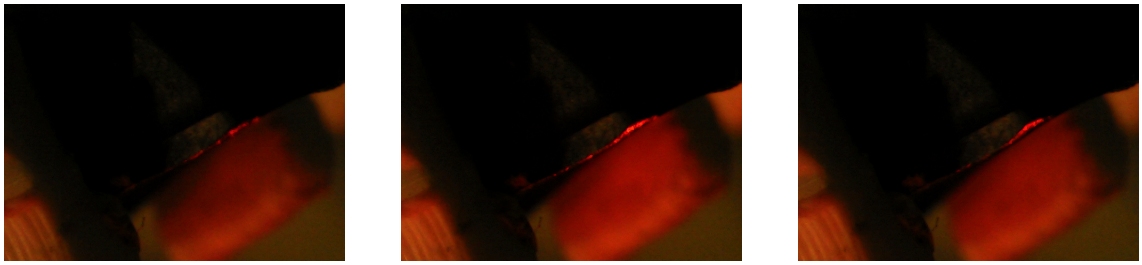

Figure 3.14: Side camera view for led 8 through 10 listed from left to right.

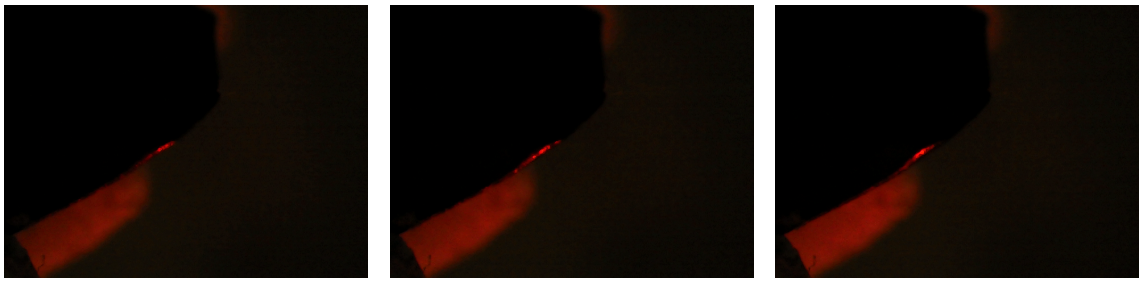

Figure 3.15: Top camera view for leds 5 through 7 listed from left to right.

cessfull because the leds didn't turn on when the photo's where taken. So the results are all black pictures with al little shadow of the insert caused by the polluting light.

By putting a delay before sending a command to the Arduino to provide the wanted lighting conditions. Although this was a very long process the results are way better than the ones from the first take on this camera setup.

The results of this test setup can be found in Figure 3.14. The insert is lighted with two corresponding leds coming from the two led strips described in 3.1.3.3. On the left is the result for led number 8; in the middle led number 9 and on the right led number 10. This lightens the worn area very good. Although the background is lighted as well and makes it harder to only see the worn area. On this we can build the first dataset but first some other camera positions are tested.

Top camera position A second test was conducted with the camera mounted a little more to the top of the inserts. This made the reflection from the worn area to the camera better. For this test the same inserts where used (batch 4 insert 1 to 5).Every pair of led is lighted separately to generate the photo's.

For this test the issue with the arduino communication was resolved by changing the input delay from the serial input reader. The following pictures where the result. Like on the previous test one picture was taken for every two leds of the strip with red light. for batch number 4 insert 3 this time with leds 5,6 and 7 turned on since the position of the camera relative to the leds changed.

On this data we can see the leds going up on the insert wear area. Which is what we tried to obtain. Now the leds are mapped to specific positions on the inserts and the amount of leds that need to be turned on for taking pictures can be reduced so no extra time is wasted.

3.2.3 Created datasets

The full datasets will be discussed in this page where firstly the dataset is documented, after that the tests that lead to this dataset are discussed.

3.2.3.1 Birthday dataset

The birthday dataset was created on 27/11/2020 with a part of the given inserts for every possible color and led setting where pictures are taken from inserts using the two separate led strips where every led is turned on separately. This is done for white, red, green and blue colors as listed below. This results in a total of 91 images per insert side.

- 1 picture with all leds on white
- 30 pictures with red lighting; 15 of led strip A and 15 of led strip B
- 30 pictures with blue lighting; 15 of led strip A and 15 of led strip B
- 30 pictures with green lighting; 15 of led strip A and 15 of led strip B

Here two ledstrips where mounted and pointed at the photographed insert. The brightness is set to 80% for all LED's to make sure to not clip against the saturation values for the pixels. The inserts where attached to the wheel with black clips 3D printed with PETG. This was chosen above white clips to lower the light reflections into the camera. This was a problem in previous setups. Also a sturdy camera mount was fabricated out off metal profiles and 3D printed parts to get better notice of the placement of the camera opposed to the insert.

The image taking process took about 1 minute per batch because of the amount of pictures taken. Since time was limited and the setup wasn't yet perfect we decided to only run 60 inserts through it. These where from batches 1 to 11.

Sample pictures of this dataset can be found in Figures 3.17 and 3.18. Where 3.17 are images from led strip 1 and 3.18 are images from led strip 2. We can see that led strip 1 wasn't configured well thus it resulted in all black pictures. For led strip one we can asses the use of colors. Only white and red are really visible, blue and green are not visible on the images thus these colors won't be used.

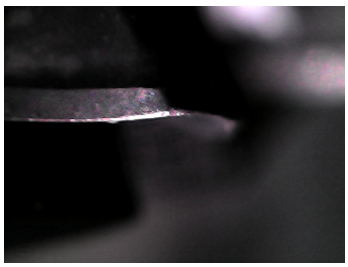

Figure 3.16: Fully lit example for insert 5 from batch 3.

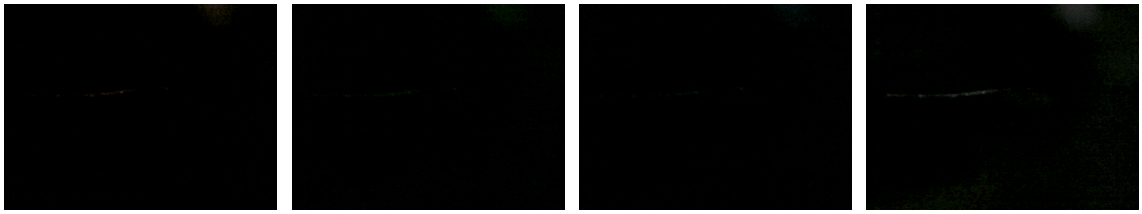

(a) Red **(b)** Green **(c)** Blue **(d)** White

Figure 3.17: Red, green, blue and white lighting on insert 5 from batch 3 led strip one. Left to right respectively

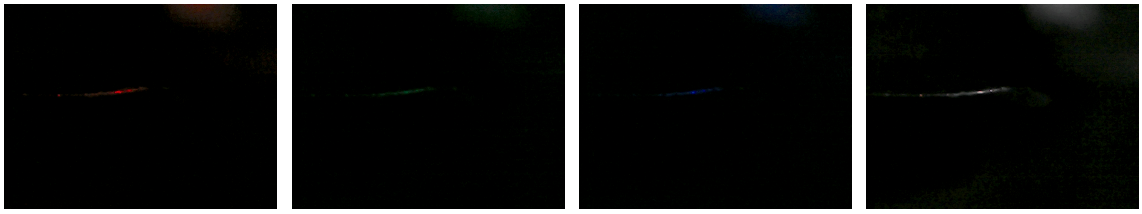

(a) Red **(b)** Green **(c)** Blue **(d)** White

Figure 3.18: Red, green, blue and white lighting on insert 5 from batch 3 led strip two. Left to right respectively.

In this dataset, there are some pictures unusable, an overview of the errors is given in Figure 3.19. As some worn areas are not even in the frame. Some to the left side (Figure3.19a) and some to the right(Figure 3.19a) side. On 3.19c we see a little plastic that was still on the insert which blocks the view of the wear area. This must be cleaned before conducting a new dataset. On 3.19d the lighting is not correctly reflected into the camera.

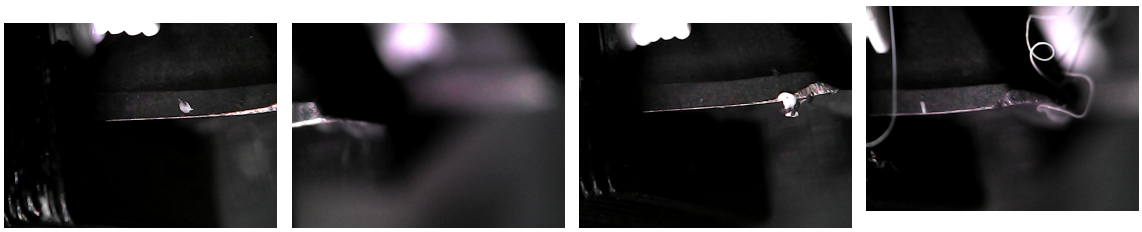

(a) Insert out of frame left. **(b)** Insert out of frame right. **(c)** Plastic on insert. **(d)** Bad lighting angle and plastic.

Figure 3.19: Errors in the Birthday dataset.

3.2.3.2 spaghetti dataset

After the Birthday dataset a new dataset was created using the things learned from that. Now the amount of LED's driven is reduced to 5 LED's. Where LED 6 to 11 is used to lighten the inserts.

Only colors white and red are used for this dataset which was discussed in 2.2.2 that the red color could have an influence on the reflection of the carbide of which the inserts are made. This was

also found in the previous dataset.

Dataset explanation For every insert, two pictures are taken. One with leds 6 to 11 on red and one with these leds white. This was experimentally found to be the best setting for reflecting the light off the worn area and into the camera.

Turning on a led to much on the upper boundary will lighten the side of the insert which isn't of much use in this paper. Turning on a led to much on the bottom boundary makes the background very bright which would provide unnecessary information. The images are separated in a folder for every insert named with batch number and insert number: batch_aaa_plate_bbb where aaa is the batch number and bbb is the insert number.

Images are named with their settings, batch number and insert number: b_aaa_p_bbb_l_006-011_color_bullet.png In this name, the following fields are used:

- aaa is the batch number;
- bbb is the plate number,
- 006-011 are the leds that turned on at the same time;
- color is the color: red or white
- bullet is the appearance of a bullet on the side of the inset and has values of b for bullet or nb for no bullet.

The dataset inserts consisted of a few different types and coatings.

Different insert types First type are the grey inserts with very visible wear. These are seen in batches 1 to 5 consistently. This type will be called grey inserts.

Than there are other inserts in batch 11 which are also grey but have a different shape on the cutting part. These will be called rounded grey inserts.

In batch 12 and 13 there are the same shape of inserts but with a black coating which results in way darker pictures as seen here on batch 13 insert 2 no bullet. These inserts are the rounded black inserts.

The next type are copper colored inserts with the rounded shape. Seen in batch 14 insert 5 no bullet.

Than we have inserts with a gold coating and hooked shape. For batch 15 insert 6 no bullet that gives the next picture:

Setup The setup used is exactly the same as on the Birthday dataset where the camera is positioned as much to the top as possible. On Figure 3.21a we can see the led strips are a little bit twisted and are positioned very close to each other. This made the reflection better and should result in better outcome of the algorithm.

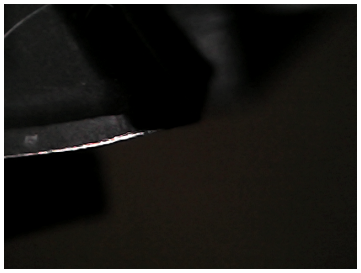

(a) Grey insert with very visible wear.

(b) Rounded grey insert.

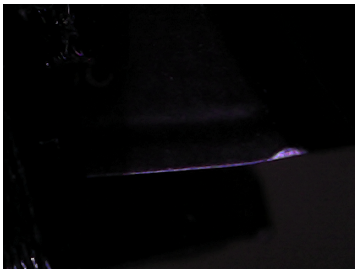

(c) Rounded black insert.

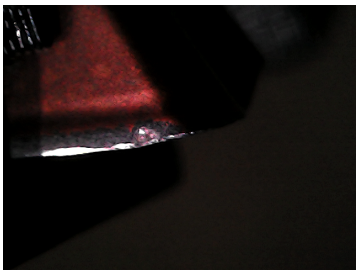

(d) Copper coloured insert.

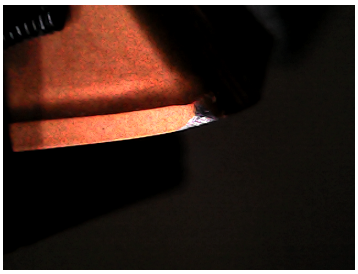

(e) Gold coloured insert.

(a) Setup with twisted led strips.

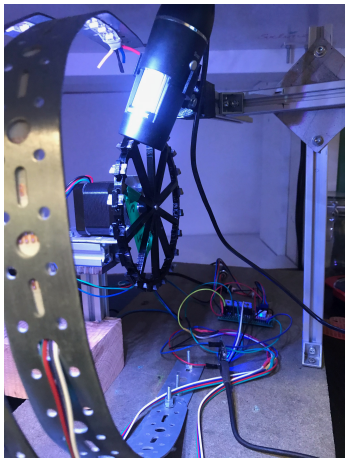

(b) Test setup camera angle more to top.

Figure 3.21: Overview of setup for the Spaghetti dataset.

The camera angle is kept the same a little to the top and very close to the inserts as seen on Figure 3.21b.

Through the whole dataset the direct light coming from other sources eg. the light of the room was blocked to have full control of the lighting conditions.

Results Underneath are some pictures of good examples in the dataset.

Figure 3.22 shows two pictures of batch 3 insert 6. These where lid with red light in 3.22a and white light in 3.22b. Here is a nice wear shown and lighted. However if we zoom in to the picture the top part of the wear is not lighted that well. We can also see a white piece of the insert holder on the image which is providing some extra difficulties. There where also a few images not fully in focus in this dataset. The discussion of these difficulties will be bespoken in section 3.3.

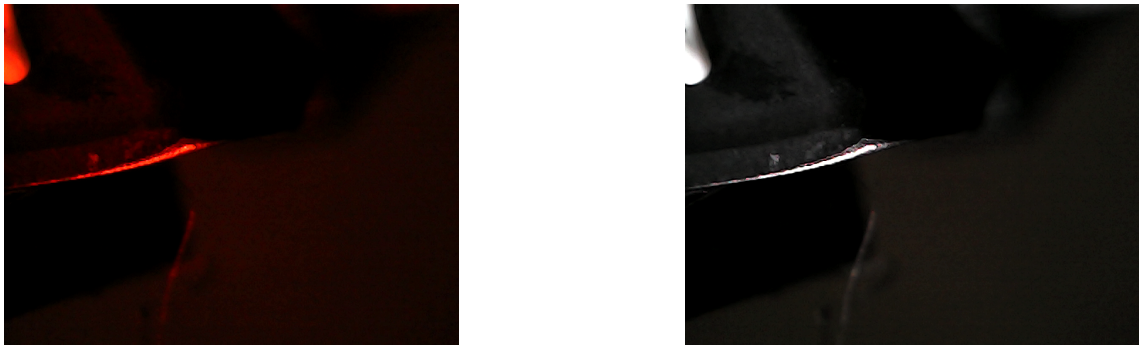

(a) Red light **(b)** White light

Figure 3.22: Example images for red and white light for spaghetti dataset.

3.3 Vision algorithms

To test the camera setup, a classification model is made where inserts will be classified into three classes. The program overview is given in Figure 3.23. This section will be following the path on the figure starting with data organisation, going to model creation and anding with training and testing. The results obtained with this algorithm will be analysed in chapter 4.

3.3.1 Data organisation

Before anything can be learned the data must be adjusted to provide a proper input to the model architectures. All these models require an input image of 224 by 224 pixels. First the labels are obtained from the labels file. Then the files are sorted into folders based on the class and function. After that the transformations on the images are defined to finally create a dataset.

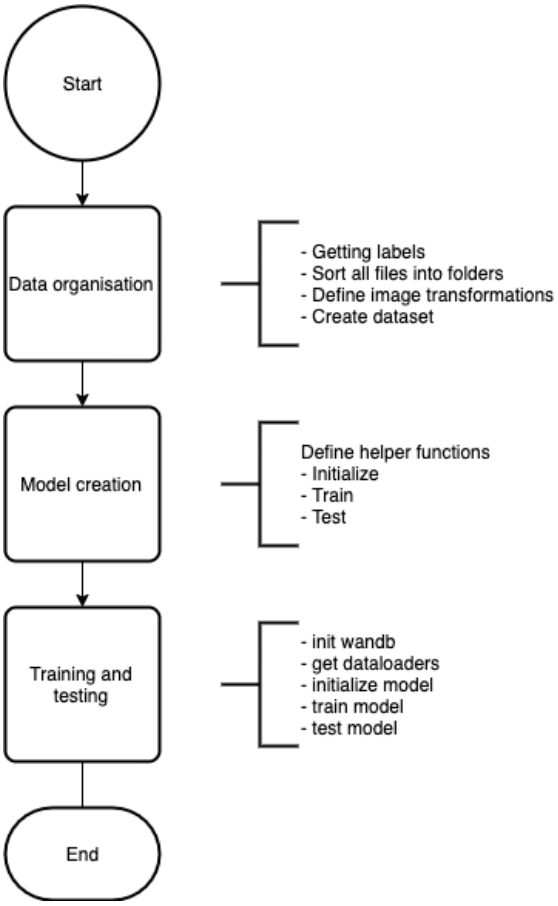

Figure 3.23: Program sequention for testing different setups.

3.3.1.1 Getting labels

All labels where saved in an Excel file which was exported to the csv file type. The file was loaded using the pandas library for data analysis (McKinney and Team, 2015). This file includes following columns for every insert:

1. Batch number (bn): provides the number of the batch, each batch consists of 10 inserts.
2. Insert number (pn): The number of the insert in the batch in range 1 to 10.
3. Bullet (b): Wether or not the side of insert has a ”bullet” mark on it. An example is given in Figure 3.11
4. Folder name: The name of the folder where the images of this insert are saved.
5. Image name: Name of the image taken for the second handmade dataset. This field doesn't serve for the other datasets.
6. Value: The measured wear value in μm.

3.3.1.2 Sorting images

The labels from 3.3.1.1 can now be used to divide images into the needed classes. For this task we will iterate over all possible images and decide to what set every image belongs and what class its value represents.

For every image there will be decided whether is goes in the training set, the test set or the validation set. The training set will hold 70% of the images, the validation set will contain 20% of the images. The remaining images will represent the test set which will be 10% of all data.

A random number will be generated between 1 and 3 which will represent one of these sets. According to this number the image belongs to a specific set. When a set is filled so it represents the amount specified by the percentage, the random number generator will only generate two numbers representing the remaining sets and so on.

When the set is declared, the image must be divided into the three classes. This will be done by comparing the wear value of the image to two set limits. A lower limit of 130 μm and an upper limit of 230 μm. The division is given below:

- Class 1: Low wear between 0 μm and 130 μm
- Class 2: Medium wear between 130 μm and 230 μm
- Class 3: High wear between 230 μm and 1000 μm

Now the set and class are known so the given image can be saved in a folder. The resulting folder structure looks like this:

Table 3.1 Overview of folder structure.

Train	Test	Validation
Low	Low	Low
Medium	Medium	Medium
High	High	High

Figure 3.24 shows the distribution of the classes for the first five batches in 3.24a and the distribution for all data in 3.24b. The class distribution should be 1/3 in the best case. The first graph shows a distribution which is close enough to this optimal distribution but in the second graph we see the distribution is far from even which must be taken into account when analysing the results.

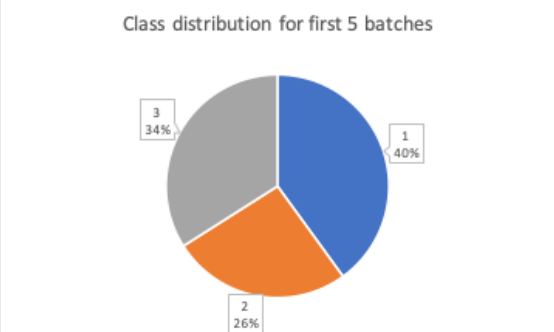

(a) Class distribution for the inserts in batch 1 to 5.

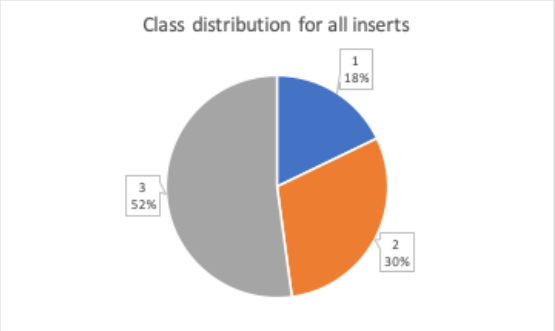

(b) Class distribution for all inserts.

Figure 3.24: Class distributions for the inserts used for the algorithm training and testing

3.3.1.3 Image transformations

To provide more data from the images we already have, data augmentation is used where the images will be transformed and will then also be used as training and validation images. These transformations consist of a rotation between 0 and 4 degrees, a translation in both x and y direction of 0.2 times the width or height respectively and a shear of 0.1 also in both directions. After these transformation the images are rescaled to a 224 by 224 resolution since this is what the model architectures expect as input resolution. The images are also normalized using the mean and standard deviation values from the Imagenet dataset (Deng et al., 2009). This can be further optimized by calculating the mean and standard deviation of the full dataset ourselves but wasn't done for these tests.

3.3.1.4 Dataset creation

With all this done a dataset can finally be created by using PyTorch's ImageFolder function from the torchvision library. (Adam et al., 2020)

3.3.2 Model creation

For the model creation a few helper functions are created. One for initialisation of different model architectures. A second one to train the model and a third to test the model after training.

3.3.2.1 Model initialisation

Every CNN architecture has a different initialisation where the input and output size must be set. This input size will be 224 pixels by 224 pixels for all architectures used for the setup validation. The output size is a vector of size 3 which will store the probability for every class. Since this initialisation step is clustered in one function, more model architectures can be added easily. The following architectures are already implemented:

- Resnet18
- Alexnet
- VGG11_bn
- Squeezenet
- Densenet

An initialisation for Inception v3 was also implemented as this was said to be well performing by Xu et al. (2019) in section 2.3.4 but this did not seem to work. Due to time limitations the issue wasn't solved but will be solved in further researches on the value prediction.

3.3.2.2 Define training

The training of a CNN happens in two phases: a training phase and a validation phase. First the model will be trained with images gathered from one batch of images. This training phase will let some pictures of the batch go through the network and will adjust the weights of that network using back propagation. The back propagation can be done using different optimizers which will define how the weights are adjusted in function off the loss between the output of the model and the ground truth. As optimizer Stochastic Gradient Descent (SGD) is used. Cross entropy loss is used to calculate the loss between the output and the ground truth.

When the training phase is done, the training takes some images from the validation set to verify or validate the weights set by the training phase. This validation will check how the model reacts to pictures it wasn't trained on and therefore shows how the model works for general cases.

The two described phases will be repeated for every epoch which will represent the duration of the training.

During the whole process of training some values are logged to be able to check the training after it is done. For this purpose the training accuracy and loss are calculated and saved and the same

values are stored for the validation phase. These values are logged using Weights and Biases (wandb) (Biewald, 2020) which will transform these logs into graphs and other useful data.

3.3.2.3 Define testing

In the data organisation section (3.3.1) a separate test set of images is created, this will be used to evaluate the model. For this evaluation every picture from the test set will go through it and the output will be compared to the ground truth. To log these tests, Weights and Biases is used as well where it saves some test pictures with their outputted class and the ground truth.

3.3.3 Training and testing

Finally the above functions will be used to actually train and test the model's performance. For the training all data will be pushed to a GPU from Google Colaboratory. To perform the training a sweep is created on wandb which will generate a set of hyper parameters that will be passed on to the training function of the model. With these parameters a dataloader is created that will generate image batches using the defined dataset from section 3.3.1.4. This dataset will contain a specified amount of images defined by the batch size parameter. After this the model gets initialized, an optimizer is created as well as a loss criterion that will define the back propagation steps. Then the model is trained for a set amount of epochs hereafter the model is tested and the results are written to wandb.

Chapter 4

Results

4.1 Setup

A fully adjustable setup is created and used to create datasets.

To obtain results all datasets are tested with the described program from **??**. The output is listed for every dataset starting with the second handmade dataset than the results of the Birthday dataset are listed. The Spaghetti dataset is listed third and finally the second handmade dataset is compared with the spaghetti dataset.

The results and graphs where obtained with Google Colab on a regular GPU and for the processing of the logs Weights and Biases was used.

4.2 Second handmade dataset results

The second handmade dataset was created in 3.2.1.2. An example of this dataset is given in Figure 4.1. For this dataset 905 test runs where conducted with different parameters to obtain the best possible results. First an overview is given on the overall performance by listing the five best runs. Next these results are compared for the different initialized model architectures as described in 3.3.2.1. The influences of parameters are discussed to conclude with a few example results on the test set.

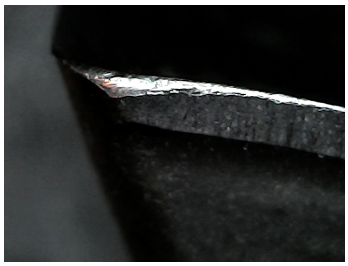

Figure 4.1: Example of second handmade dataset batch 3 insert 4.

4.2.1 overall results for the five best runs.

For the five best results we get up to a validation accuracy of 100%, a test accuracy of 100% and a train accuracy of 97%. This is almost a perfect result for the classification model. Bear in mind that this is just performed on 100 pictures separated in three categories: train, validation and test. These categories have 71, 20 and 9 pictures respectively. Since there are so little test pictures the test score is not fully valid but we can conclude this is a very good test run.

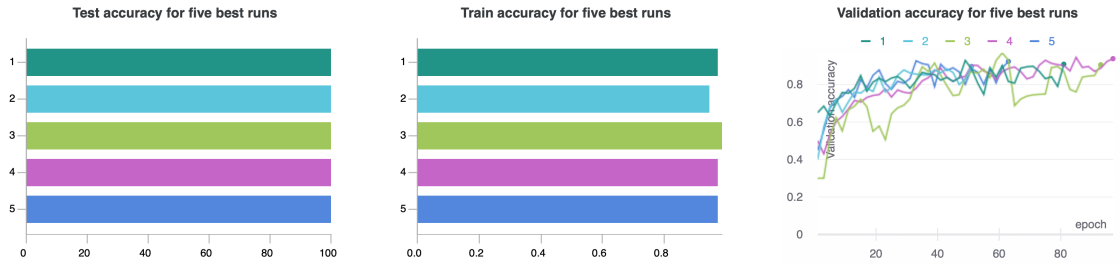

(a) Test accuracy **(b)** Train accuracy **(c)** Validation accuracy

Figure 4.2: Test, train and validation accuracy for five best runs with second handmade dataset.

4.2.2 Comparison between the different model architectures

To get a better overview on how different architectures perform for the dataset, we compare the main results for al these tested architectures. Starting with Test accuracy on these models, later the validation accuracy is discussed.

4.2.2.1 Test accuracy

The test accuracy on 9 pictures from different classes that were randomly picked is really high. For 4 out of 5 model architectures the test accuracy is 100% so all inserts where predicted correctly. Densenet is performing a little worse with an accuracy of 89% what means that only one image wasn't predicted correctly. This is the result of testing 905 different parameters during training of the model. VGG11_bn is showing a smaller difference between the minimum test accuracy of all tests and the maximum accuracy of all tests. For now the VGG11_bn is the best model architecture based on the test accuracy.

A simple confusion matrix is created for 9 runs with 9 images each. top to bottom truth left to right predicted

Compare this with the distribution and values. The border between low and medium is at 130 micrometer and the border between Medium and High wear is at 230 micrometer. Since these limits are just a number there are a lot of values just before and just after the limit. This makes is hard for the algorithm and isn't even possible to see a difference between these for the human eye.

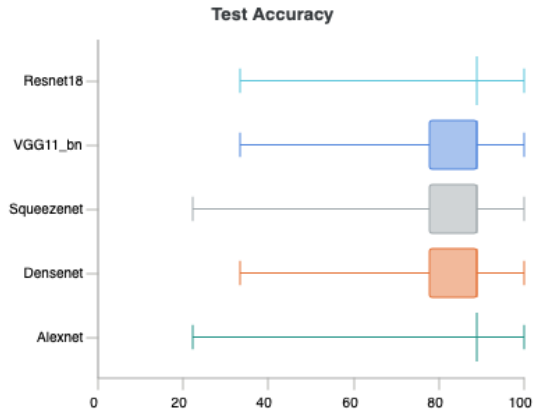

Figure 4.3: Test accuracy for different model architectures with maximum and minimum values.

Table 4.1 Confusion matrix for tests of the second handmade dataset.

	Low	Medium	High
Low	x	2	0
Medium	2	x	5
High	0	2	x

The confusion shows that the predictions between Medium and High are the most difficult. What we can also find is that there are no predictions totally wrong where High wear is predicted as low or vice versa.

4.2.2.2 Validation accuracy

The validation accuracy is plotted in function of the epochs which gives an overview of how the training went. In the beginning there is a learning curve and at the end the graph stabilises. This means the training got a good amount of epochs to reach the optimal point.

This graph is smoothed to create a better overview. The shadows behind are the standard deviation for each model. Some models tend to train faster to a higher validation accuracy like Alexnet and Squeezenet. However this doesn't result in a better outcome for Alexnet where the median scores worse.

Validation accuracy for best runs is given in table ... There are two measurement methods we can use namely the highest test accuracy and the highes validation accuracy. In the first column the highest reached validation accuracy is given for each model. We can see here that more models reach 100% validation accuracy which should translate into a good generalisation. The results of the generalisation are given in the second column. Here the numbers represent the highest values for validation accuracy from the runs with the highest values for test accuracy. Or the table of all runs is sorted on test accuracy and the validation accuracy is taken from the first five runs. Here we can see the order isn't changed, there is just 5% lost in accuracy. It declares the link between validation accuracy and test accuracy.

Model name	Validation Accuracy	Validation accuracy sorted on test accuracy
Alexnet	100%	100%
Resnet 18	100%	95%
Squeezenet	100%	95%
VGG11_bn	95%	90%
Densenet	95%	90%

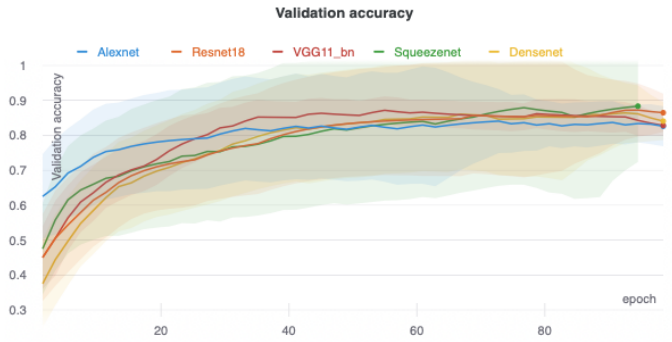

Figure 4.4: Best validation accuracy for different model architectures.

4.2.3 Influence of Transfer learning on the results

The influence of transfer learning from the imagenet dataset is visualised in the following graphs. First the test accuracy is plotted for every model architecture and with transfer learning (TL) or without transfer learning (No TL) in Figure 4.5a. Here the results are almost identical for the two different settings. The maximum test accuracy measured is 100% for every model. The distributions changed a little bit which may be caused by the amount of test runs conducted for that model architecture.

The second graph on Figure 4.5b plots the validation accuracy for the different networks with or without transfer learning. From these boxplots we can see that Alexnet benefits from transfer learning. What would be due to the architectures small amount of parameters. Squeezenet and Resnet 18 actually get worse results with transfer learning opposed to traning without transfer learning.

4.2.4 Other influences of parameters

The settings for the best 40 runs are visualized in Figure4.6. For every model architecture some different hyperparameters are listed with their values for different training runs. From left to right we see the model name, the amount of epochs for the training, the batch size, whether or not transfer learning is used and finally the learning rate. Since this graph shows the top 40 runs the amount of runs starting from a single model name defines its presence in this top 40. Squeezenet and Resnet18 are represented by a lot of runs where the most green lines start from Squeezenet. This green lines indicate a validation accuracy of more than 80% for that run.

Other things we can learn from this graph are:

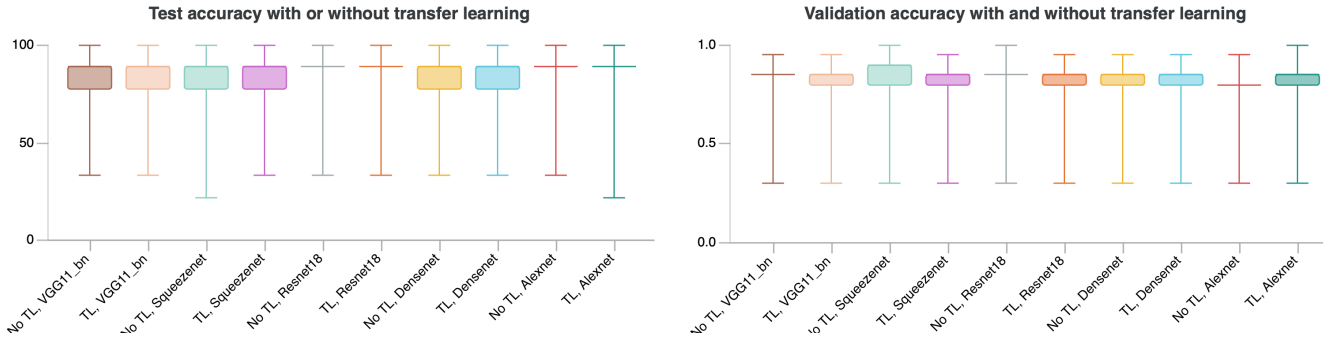

(a) Test accuracy **(b)** Validation accuracy

Figure 4.5: Validation and test accuracy box plot for different model architectures with or without transfer learning (TL).

- The epochs have a significant contribution to the validation accuracy where the amount of epochs can be finetuned between 30 epochs and 47 epochs for best results.
- A batch size between 10 and 4 seems good but doesn't contribute that much to the final results since the spread of runs across the different batch sizes is pretty even.
- There are more runs in the top 40 that doesn't use transfer learning. This means the transfer learning doesn't affect the results in a positive way for the most part.
- The learning rate used for adjusting the weights can differ highly from one run to the other. No points on the learning rate graph actually are significantly more populated than others. The learning rate can be set to higher and lower values for further testing.

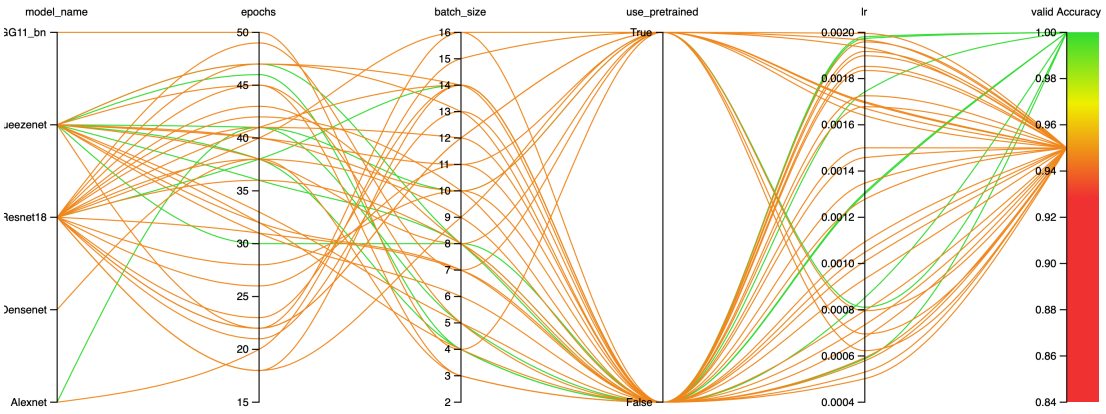

Figure 4.6: Parameter influence on validation accuracy.

4.2.5 test images

Use these images to show what high wear, medium wear and low wear looks like? and leave this section out Since the test accuracy was so high only a few images were mispredicted

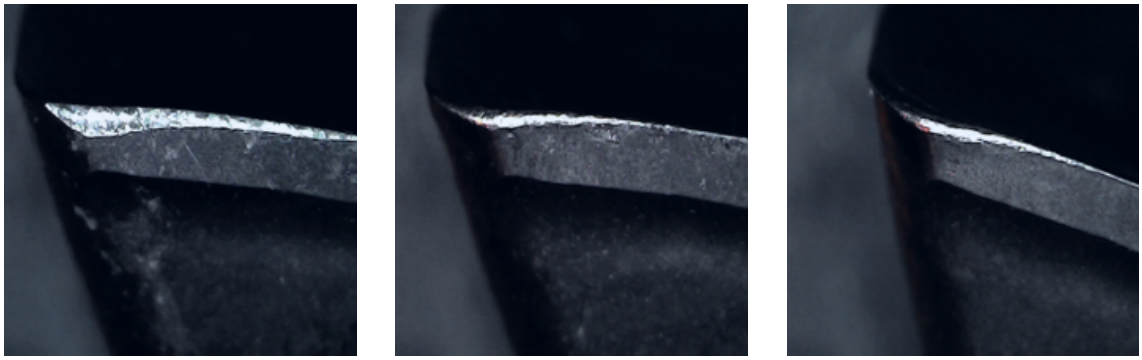

(a) Truth: High
Predicted: High

(b) Truth: Medium
Predicted: Medium

(c) Truth: Low
Predicted: Low

Figure 4.7: Result images with their results.

4.3 Birthday dataset results

For the birthday dataset there are no results available because the dataset was not considered as good which was discussed in 3.2.3.1.

4.4 Spaghetti dataset results

The spaghetti dataset was the first dataset to capture all of the currently available tool inserts. Here the different insert types are all in one dataset where white as well as red lighting was used. 158 runs where completed with different parameters to generate the following results. For this third dataset the overall results are discussed in the first section where we take a look at the five best runs. After the general results we dive deeper into the different model architectures. After which some differences will be discussed.

4.4.1 Overall results for five best runs

The five best results are discussed to get a quick overview of the performance of this dataset on the chosen model architectures. The test accuracy for the five best runs is shown in Figure 4.8a. The maximum test accuracy is 82.1%, this value is not as expected. To dive deeper in the training we take a look at the training accuracy in Figure 4.8b the training accuracy is very high near 100%. The high training accuracy means the training pictures get predicted correctly but the other general pictures get predicted wrong in 20% of the cases. To take a deeper look into this difference

between testing and training accuracy we take a look at the validation accuracy during training. If the training accuracy would increment and the validation accuracy would decrement after a time the model might be over fitting. Figure 4.8c shows the training and validation accuracy during training. There is no overfitting seen on this graph so the model just isn't powerful for the task or the size of the dataset is not large enough.

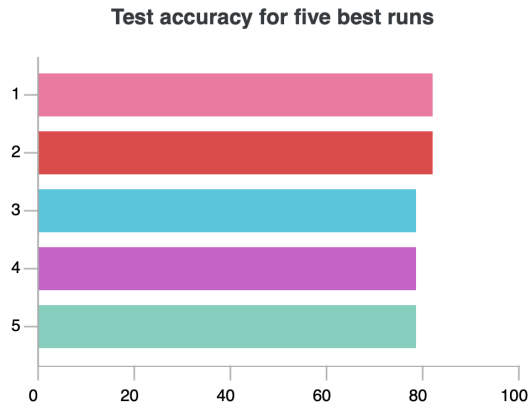

(a) Test accuracy

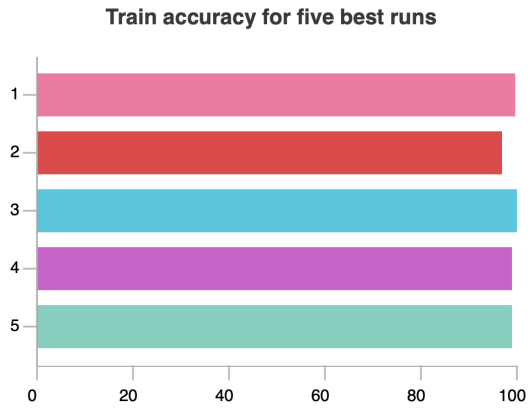

(b) Train accuracy

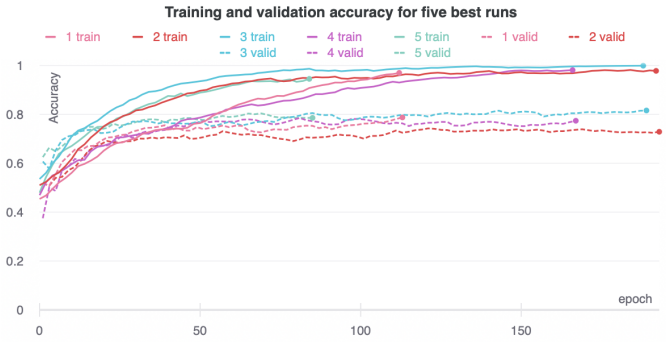

(c) Training and validation accuracy

Figure 4.8: Test, train and validation accuracy for the five best runs based on their test accuracy scores.

4.4.2 comparison between different model architectures

Just like the Second handmade dataset results the different model architectures are compared. The test accuracy, validation accuracy and influence of transfer learning are analysed.

4.4.2.1 Test accuracy

On the first graph the test best test accuracy for every model is plotted. Here Densenet received the best accuracy for predicting the wear class of images on the test set. 78 percent of images were correctly predicted. The other architectures aren't far behind on the accuracy with 75 percent. Resnet 18 on the other hand is performing worse with a test accuracy of only 67 percent. On this first opinion Densenet seems to be the best model for this classification task.

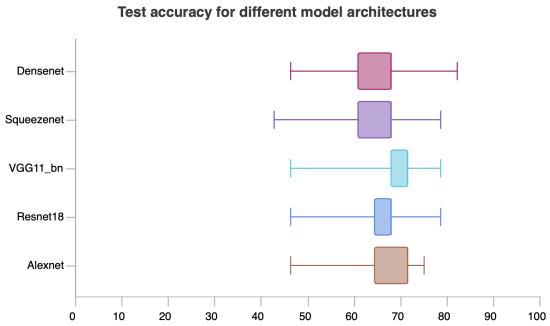

Figure 4.9: Test accuracy

4.4.3 Validation Accuracy

To further check the performance of the models a graph is shown in figure below. Here the validation accuracy is plotted for every model with its minima and maxima in shadow. There is not much of an inclining curve to this graph where normally the graph would go up in the first half and stabilise at the end.

Squeezenet and VGG11_bn seem to have trained to the highest validation accuracy of 82%. This is an indication on how well the model will react on new images like the images of the test set. After those two Densenet with an accuracy of 78%, Alexnet with an accuracy of 75% and finally Resnet 18 with an accuracy of 73%. Here must be noticed that Resnet 18 only got tested in 3 different parameter configurations whereas the others where optimized a bit more.

Table ... shows the results for the different datasets where the test and validation accuracy predict almost the same order for best model architecture. VGG11_bn and Densenet take the lead here. These networks are complexer with more layers and more parameters.

Model name	Validation Accuracy	Validation accuracy sorted on test accuracy
VGG11_bn	84%	82%
Densenet	84%	82%
Alexnet	82%	82%
Squeezenet	82%	78%
Resnet 18	80%	80%

Table 4.2 Validation accuracy plotted for best model per architecture. In first column sorted on best validation accuracy, in second column sorted on best test accuracy.

4.4.4 Influence of transfer learning on the results

For comparison with the second handmade dataset the transfer learning influence is plotted in Figure 4.11a for the test and validation accuracy. Overall Transfer learning seems to have an effect on this dataset where the runs with transfer learning score on average 2% better and the maximum result is 5% better which is a significant improvement over the runs without transfer learning.

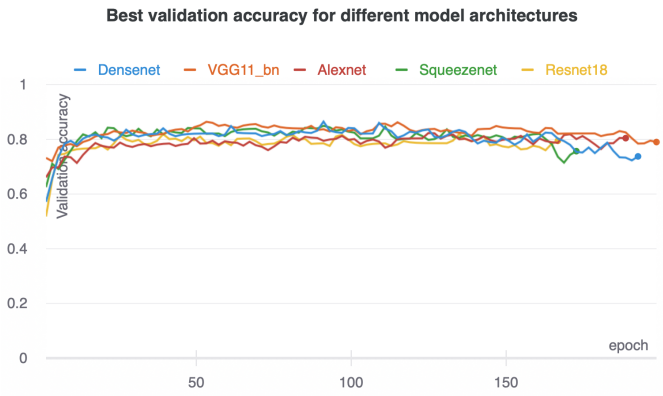

Figure 4.10: Best validation accuracy for different model architectures plotted in relation to the amount of epochs.

The same difference is also compared for all different model architectures in Figure 4.11b. Squeezenet, Resnet 18, Densenet and Alexnet all benfit from transfer learning. VGG11_bn on the other hand doesn't benefit from transfer learning and produces the same results for both settings.

As there are significant differences in the results for training with or without transfer learning the training of the models is examined. First the median and standard deviation of the validation accuracy during training is plotted in Figure 4.11c, secondly the train accuracy is plotted in Figure 4.11d. For the validation accuracy the learning curve with transfer learning inclines a bit before the curve for the training without transfer learning. using a pre-trained network speeds up the initialisation of the network but also uses more epochs to finish the training. For the training accuracy this curve there is no significant difference.

4.4.5 Red vs White

For further investigation of the lighting color effects on the results, the median and standard deviation of the test and validation accuracy are plotted in Figure 4.12a and 4.12b. For the validation accuracy there is a small difference of 4% between the two curves where the white lighting seems to perform better. On the test accuracy there is a similar outcome for the median results but the best results got achieved by the dataset with red lighting.

4.4.6 training runs

On figure 4.13 different runs with different parameters are displayed. Here can be seen that more green lines start from the white dataset. This is in line with previous findings where was stated that the white dataset performed better on average. The batch size can be finetuned between 16 and 2. The amount of epochs van be increased in an attempt to better the results, however on Figure 4.8c the validation accuracy seems to be stable at the end where adding more epochs wouldn't change much on the results. The learning rate van be kept between 0 and 0.002. Using transfer learning isn't a deciding factor for good results.

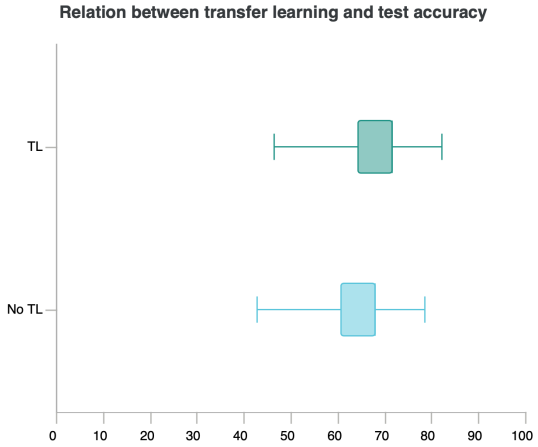

(a) Test accuracy for all runs with and without transfer learning.

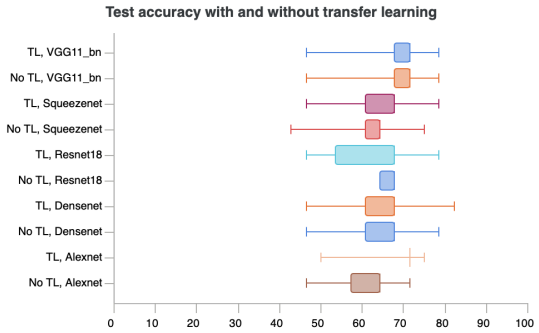

(b) Test accuracy with or without transfer learning for different model architectures.

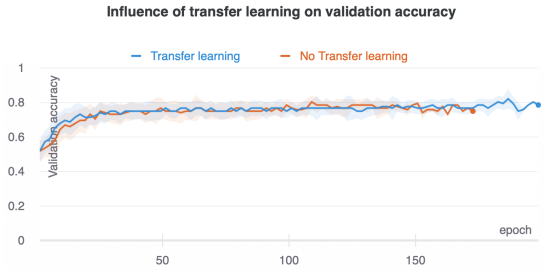

(c) Validation accuracy

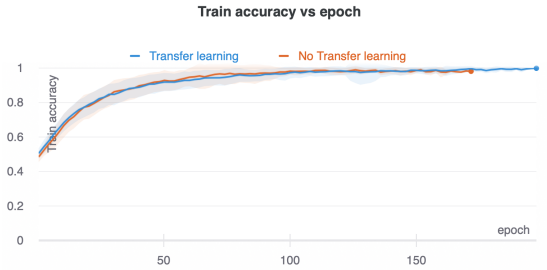

(d) Training accuracy

Figure 4.11: Test accuracy for models trained with and without transfer learning. In picture a) a general overview of all performed tests. in picture b) a comparison between different model architectures. Picture c and d provide the differences during training for validation accuracy and training accuracy respectively.

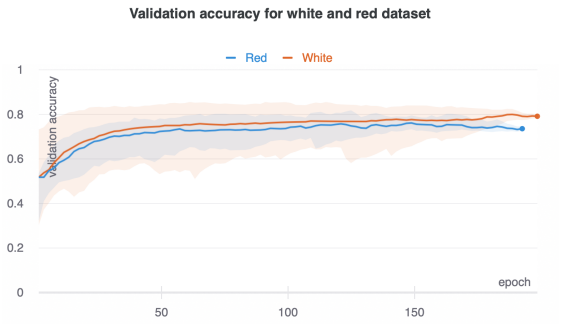

(a) Test accuracy.

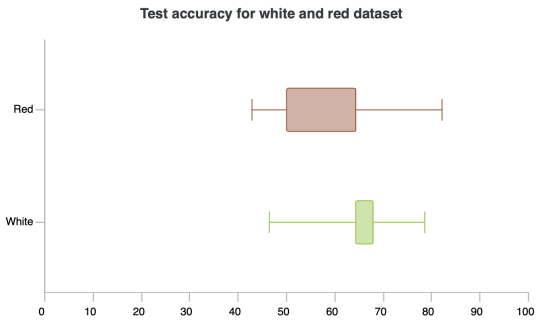

(b) Validation accuracy

Figure 4.12: Test and validation accuracy for a different led color.

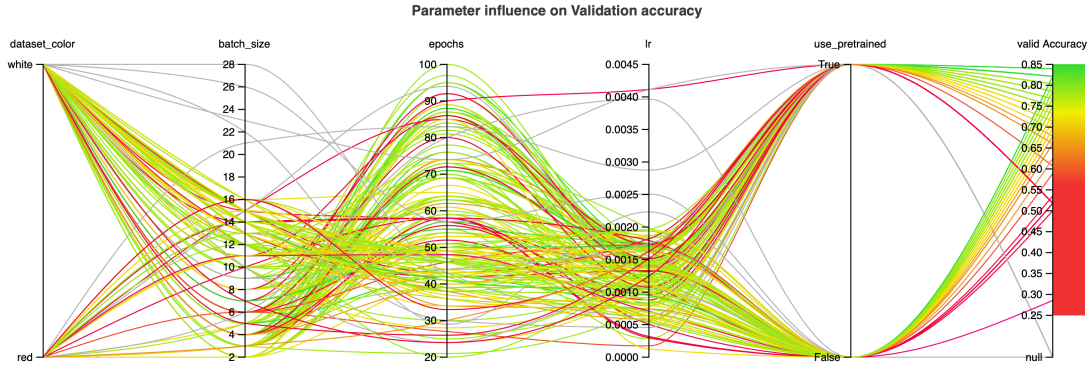

Figure 4.13: Parameter influence on validation accuracy.

4.4.7 Test images

To illustrate the results, some test images from the white lighted part of the dataset are listed in Figure 4.14. One error is given in Figure 4.14c Where high wear was predicted for a medium wear insert. No hard mistakes where resulting in this test set where low wear was predicted as high wear or the other way.

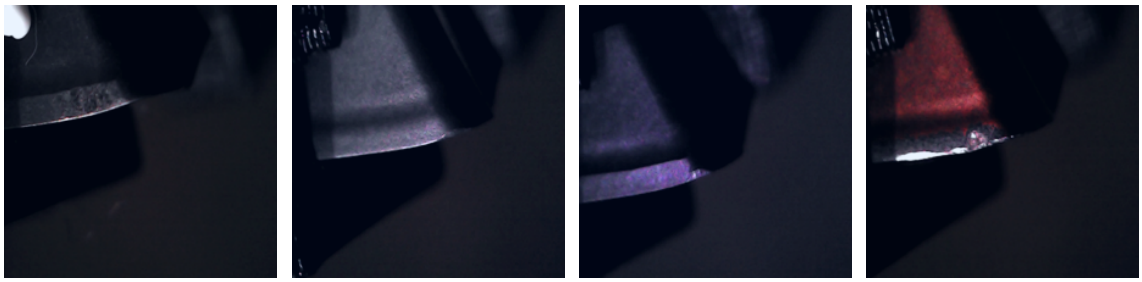

(a) Truth: Low
Predicted: Low

(b) Truth: Medium
Predicted: Medium

(c) Truth: Medium
Predicted: High

(d) Truth: High
Predicted: High

Figure 4.14: Images with predictions from the spaghetti dataset with white lighting.

For the test set with red lighting are also images listed in Figure 4.15. Figure 4.15c displays an error where a medium wear inset was predicted as high wear. This also is not a big error.

4.5 Spaghetti dataset compared with second handmade dataset

If we compare the results from the spaghetti dataset with the results that where obtained from the second handmade dataset, these results aren't as expected since the amount of data in the dataset is more than doubled but the results for the test are worse. To give an overview of the dataset three inserts are listed from the datasets:

- one from the second handmade dataset in Figure 4.16a

(a) Truth: Low Predicted: Low

(b) Truth: Low Predicted: Low

(c) Truth: Medium Predicted: High

(d) Truth: High Predicted: High

Figure 4.15: Images with predictions from the spaghetti dataset with white lighting.

- one from the white part of the Spaghetti dataset in Figure 4.16b
- one from the red part of the Spaghetti dataset in Figure 4.16c

(a) Image from second handmade dataset

(b) Image from Spaghetti dataset white

(c) Image from Spaghetti dataset red

For further investigation the datasets are globally compared first and after that the influence of the different model architectures on the datasets will be bespoken.

4.5.1 Global comparison

For the comparison the Spaghetti dataset is split up into a white and a red part so the results of the white part should match the results from the second handmade dataset.

First we compare the train accuracy and the validation accuracy to spot differences in the learning curve of these two datasets. For the training accuracy of Figure 4.17a we see that the second handmade dataset requires much less training epochs and increases in train accuracy much quicker. For the validation accuracy in Figure 4.17b there is a similar trend. On both figures can be noticed that the standard deviation given in shadowed color is much larger for the Spaghetti dataset what means the training runs where much more fluctuating. From these results we can conclude that the spaghetti dataset is much harder to learn. For the confirmation we look at Figure 4.17c where the test accuracy is plotted. The same can be extracted from this figure as from the orhter two. Where the second handmade dataset has less fluctuation and produced much more

consistent good results and the spaghetti dataset also reached an accuracy of 100% but has much more runs with a lower accuracy.

max accuracy for second handmade=

(a) Train accuracy

(b) Validation accuracy

(c) Test accuracy

Figure 4.17: Comparison for test, train and validation accuracy for different datasets.

If we compare the best results obtained for the second handmade dataset and the spaghetti dataset based on the validation accuracy (first column) and on the test accuracy (second column) the results seem very familiar. The same order is kepth and even the values don't differ much. Alexnet, Resnet 18 and Squeezenet can be said to be the best architectures for this problem with the smaller, simpler dataset. This table can also be compared against the table from the full spaghetti dataset where the order is basically reversed.

These results can be declared based on the Table 2.1 Alexnet, Resnet 18 and Squeezenet all have similar values for the number of parameters and depth (61.1 M, 11.7 M, 1.2 M) and (8, 18, 10) respectively. VGG11 has 123.1 M parameters and 11 layers and Densenet 121 has 7.9 M parameters and 121 layers. From this information we can conclude that a wider network with less parameters and layers produces better results for this easy problem with a small dataset. But for the more difficult problem with the Spaghetti dataset where more data is provided, the architectures with more parameters and layers like VGG11 and Densenet 121 are better.

Model name	Validation Accuracy	Validation accuracy sorted on test accuracy
Alexnet	100%	100%
Resnet 18	100%	100%
Squeezenet	100%	100%
VGG11_bn	90%	90%
Densenet	90%	90%

4.5.2 difference for different model architectures

To check the influence of the model architecture on the dataset we plot the test accuracy for every dataset and all different architectures. This is shown in Figure 4.18 where SHM stands for second handmade dataset; red stands for the red part of the spaghetti dataset and white for the white part.

The same conclusions can be taken for these models as for the global results for these datasets. The model architecture doesn't incorporate a sufficient difference in results.

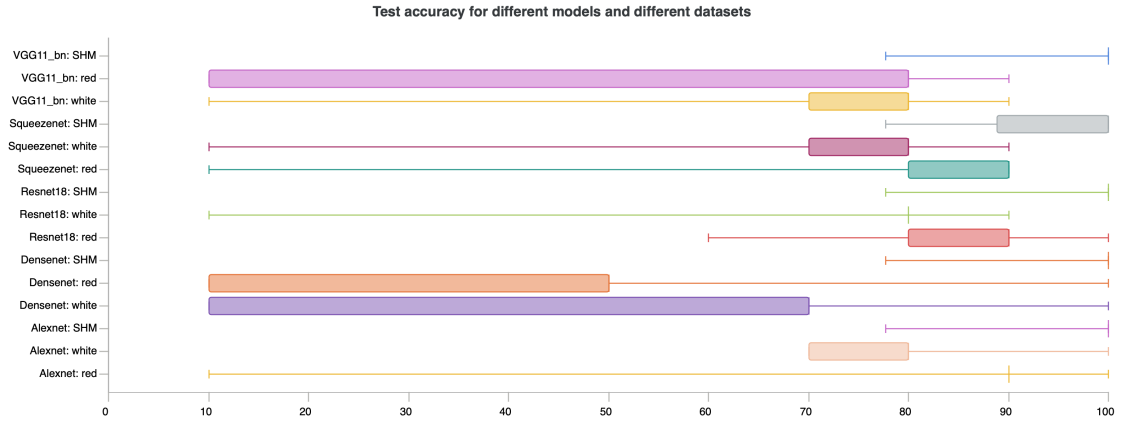

Figure 4.18: Difference in test accuracy for different datasets trained with different model architectures.

As already noted in the section about the spaghetti dataset, there are disturbances in the images where the white or black plastic from the tool holder comes into the frame. This makes it harder to separate some pictures. Secondly the position of the worn area isn't always the same like in the second handmade dataset.

To conclude: the images must be taken a bit better so less unwanted things are in the picture and the wear should be lightened in a way that makes it possible to detect the different wear areas on different inserts.

Chapter 5

Conclusion

5.1 Inleiding

De referentielijst bevat de volledige lijst van literatuur en bronnen waarnaar in de tekst wordt verwezen. Door systematisch de referentielijst aan te vullen bij het schrijven van het literatuuroverzicht gaat er achteraf geen tijd verloren aan het opnieuw opzoeken van referenties.

5.2 Referentiestijl

Voor het verwijzen naar informatiebronnen wordt gebruik gemaakt van het numerisch systeem of van het auteur-jaar systeem. Dit kies je door volgend commando in het latex bronbestand aan te passen:

- numerisch (IEEE) : `\bibliographystyle{ieee}`
- alfabetisch (APA) : `\bibliographystyle{apalike}`

Plaats je bronnen in een *bibtex* bestand (evt. via software zoals bv. Jabref Endnote of Mendeley), waarnaar je verwijst vanuit je thesis text a.d.h.v. het commando `\cite`. Enkele links naar nuttige software in deze context:

- JabRef (Open Source)
- Mendeley (Freeware)
- EndNote (Paid license)

Indien je zelf een .bibtex bestand wil aanleggen dien je volgende syntax te volgen voor een tijdschriftartikel:

```
@article{hughes2005,
title={Isogeometric analysis: CAD, finite elements, NURBS, exact geometry
and mesh refinement},
author={Hughes, Thomas JR and Cottrell, John A and Bazilevs, Yuri},
journal={Computer methods in applied mechanics and engineering},
volume={194},
number={39},
pages={4135--4195},
year={2005},
publisher={Elsevier}
}
```

Enkele voorbeelden van het gebruik van bronnen in een tekst (in APA stijl):

Recent werd het Higgs boson experimenteel vastgesteld door Aad et al. Aad et al. (2012) (syntax: `\cite{aad2012}`).

Als alternatief voor het discretiseren van een CAD model vooraleer een eindige elementenanalyse te kunnen toepassen, stellen Hughes et al. voor om de nodige elementenformulering rechtstreeks uit de NURBS beschrijving van de CAD geometrie te halen Hughes et al. (2005) (syntax: `\cite{hughes2005}`). Daarnaast introduceren ze tevens een k-iteratieve procedure als een verfijning van de geldende p- en h-iteratieve procedures in eindige elementen methoden Cottrell et al. (2009) (syntax: `\cite{cottrell2009}`).

Chapter 6

Bibliography

(2020). Raspberry pi user manual. https://www.raspberrypi.org/documentation/. Accessed: 2020-12-10.

Aad, G., Abajyan, T., Abbott, B., Abdallah, J., Khalek, S. A., Abdelalim, A., Abdinov, O., Aben, R., Abi, B., Abolins, M., et al. (2012). Observation of a new particle in the search for the standard model higgs boson with the atlas detector at the lhc. *Physics Letters B*, 716(1):1–29.

Adam, P., Sam, G., Soumith, C., and Gregory, C. (2020). Pytorch. https://pytorch.org. Accessed: 2020-12-09.

Ambadekar, P. K. and Choudhari, C. M. (2020). CNN based tool monitoring system to predict life of cutting tool. *SN Applied Sciences*.

Basnet, R. B., Shash, R., Johnson, C., Walgren, L., and Doleck, T. (2019). Towards detecting and classifying network intrusion traffic using deep learning frameworks. *J. Internet Serv. Inf. Secur.*, 9(4):1–17.

Biewald, L. (2020). Experiment tracking with weights and biases. Software available from wandb.com.

Caicedo, J. C. (2019). New color from multilayer coating applied machining tools based on tungsten carbide insert. *International Journal of Advanced Manufacturing Technology*.

Cerce, L., Pusavec, F., and Kopac, J. (2015). Novel spatial cutting tool-wear measurement system development and its evaluation. In *Procedia CIRP*.

Chandrarathne, G., Thanikasalam, K., and Pinidiyaarachchi, A. (2019). A Comprehensive Study on Deep Image Classification with Small Datasets. In *Lecture Notes in Electrical Engineering*.

Cottrell, J. A., Hughes, T. J., and Bazilevs, Y. (2009). *Isogeometric analysis: toward integration of CAD and FEA*. John Wiley & Sons.

Deng, J., Dong, W., Socher, R., Li, L.-J., Li, K., and Fei-Fei, L. (2009). ImageNet: A Large-Scale Hierarchical Image Database. In *CVPR09*.

Gu, J., Barber, G., Tung, S., and Gu, R. J. (1999). Tool life and wear mechanism of uncoated and coated milling inserts. *Wear*.

He, K., Zhang, X., Ren, S., and Sun, J. (2016). Deep residual learning for image recognition. In *Proceedings of the IEEE Computer Society Conference on Computer Vision and Pattern Recognition*.

Hughes, T. J., Cottrell, J. A., and Bazilevs, Y. (2005). Isogeometric analysis: Cad, finite elements, nurbs, exact geometry and mesh refinement. *Computer methods in applied mechanics and engineering*, 194(39):4135–4195.

I, i. (2020). Keras. `https://keras.io`. Accessed: 2020-12-09.

J, H. (2020). Fast.ai. `https://docs.fast.ai`. Accessed: 2020-12-09.

Khan, A., Sohail, A., Zahoora, U., and Qureshi, A. S. (2020). A survey of the recent architectures of deep convolutional neural networks. *Artificial Intelligence Review*, 53(8):5455–5516.

Krizhevsky, A., Sutskever, I., and Hinton, G. E. (2017). ImageNet classification with deep convolutional neural networks. *Communications of the ACM*.

Li, W., Singh, H. M., and Guo, Y. B. (2013). An online optical system for inspecting tool condition in milling of H13 tool steel and in 718 alloy. *International Journal of Advanced Manufacturing Technology*.

Ma, J., Luo, D., Liao, X., Zhang, Z., Huang, Y., and Lu, J. (2020). Tool wear mechanism and prediction in milling TC18 titanium alloy using deep learning. *Measurement: Journal of the International Measurement Confederation*.

McKinney, W. and Team, P. D. (2015). *Pandas - Powerful Python Data Analysis Toolkit*.

Pagani, L., Parenti, P., Cataldo, S., Scott, P. J., and Annoni, M. (2020). Indirect cutting tool wear classification using deep learning and chip colour analysis. *International Journal of Advanced Manufacturing Technology*.

Schmitt, R., Cai, Y., and Pavim, A. (2012). Machine Vision System for Inspecting Flank Wear on Cutting Tools. *ACEEE International Journal on Control System and Instrumentation*.

Simonyan, K. and Zisserman, A. (2015). Very deep convolutional networks for large-scale image recognition. In *3rd International Conference on Learning Representations, ICLR 2015 - Conference Track Proceedings*.

Xu, X., Zheng, H., Guo, Z., Wu, X., and Zheng, Z. (2019). SDD-CNN: Small data-driven convolution neural networks for subtle roller defect inspection. *Applied Sciences (Switzerland)*, 9(7).

FACULTY OF ENGINEERING TECHNOLOGY
DE NAYER (SINT-KATELIJNE-WAVER) CAMPUS
Jan De Nayerlaan 5
2860 SINT-KATELIJNE-WAVER, België
tel. + 32 16 30 10 30
fet.denayer@kuleuven.be
www.fet.kuleuven.be